On mass quantities of gravity frames in building structures

Bernardino D'Amico[a,b,*], Francesco Pomponi[a,b]

[a] *REBEL (Resource Efficient Built Environment Lab)*
[b] *School of Engineering and the Built Environment, Edinburgh Napier University, UK*

Abstract

This paper introduces a numerical study aimed at analysing and quantifying existing correlations between structural masses of the gravity frame in building structures (i.e. excluding lateral load resisting system) and some key basic design variables, such as bay areas of the frame layout, magnitude of floor loads and (main) structural material. Three material options are considered, namely: reinforced concrete, steel and engineered timber. A total of 31'380 different structural frame designs are parametrically generated and analysed to obtain a population of design data points that express the amounts of structural masses per unit of floor area. Least squares and quantile regression analyses have been utilised on the numerically generated sample population to evaluate any existing statistical trend between design variables and mass quantities. The set of regression coefficients so obtained is eventually organised into a tabular format, which allows for immediate estimations of the structural mass quantities (along with their uncertainty ranges) at early stage of the structural design process. Such a table of coefficients represents the main finding of this work, as it can be straightforwardly combined with existing databases of embodied GHG and energy coefficients, therefore providing an effective estimation tool, for both practitioners and researchers, to quickly assess how both layout and load configurations affect the environmental impacts of their frame design.

Keywords: buildings, frame, structures, design, carbon dioxide, mass

1. Introduction

Building construction is a significant contributor to worldwide consumption of natural resources and it is responsible for a great share of greenhouse gas emissions (GHGs). It is estimated that 39% of global energy-related carbon dioxised equivalent (CO_{2e}) emissions and 36% of final energy use are attributable to the building sector alone [1]. Improving the operational efficiency of buildings has been the major focus for research,

*Corresponding author
Email addresses: b.damico@napier.ac.uk (Bernardino D'Amico), f.pomponi@napier.ac.uk (Francesco Pomponi)

practitioners and policy makers in the last few decades. Yet, as buildings become more efficient to manage, maintain and operate, the embodied energy and greenhouse emissions, will account for the greatest share of the building whole-life impacts [2, 3, 4], especially considering that the most energy-demanding and GHG-intensive activities are those associated with the so called cradle-to-gate stage, i.e. raw material extraction and transportation, as well as processing and manufacturing [5]. Specifically, the structure often constitutes a substantial share of the entire building mass, therefore affecting significantly the embodied externalities of the building's whole life cycle [6, 7].

Among the strategies to mitigate the embodied impacts of building structures, recent research has focused on understanding how to improve the way structures are designed in the first place: for instance, achieving material efficiency [8] by exploring shape-resistant structural systems [9, 10], or developing Computer-Aided-Design (CAD) methods to maximise the potential for deconstruction and reuse of structural components [11, 12]. Others focused on identifying the main drivers leading design practitioners to over-specification of section sizes [13, 14] (and thus, to unnecesary use of material) as well as pointing out to optimisation methods as an effective tool to achieve material efficiency in practice [15, 16, 17]. A common denominator emerging from these studies is the requirement for structural engineers to account for the environmental implications of their design choices.

Construction cost is one of the main criteria in structural design practice, encompassing the context-specific constraints/requirements of the project at hand, and driving engineers toward a range of preferred design solutions. In addition to the monetary cost, the environmental 'cost' is becoming increasingly relevant, and this has led in recent years to a wealth of research aimed at quantifying the embodied energy and carbon dioxide of buildings [18, 19, 20] and structures [21, 22, 23, 24] along with their uncertainty [25, 26]. Software database and libraries [27, 28] initially developed in the context of Life Cycle Assessment (LCA) are now also used within the building and structural engineering communities.

It is worth stressing the importance of paying the same attention to embodied GHG coefficients as it is done to structural masses and this is often times not done in the engineering communities. Instead, inventories such as the ICE [29] which are not peer-reviewed, lacks transparency, and mix and average values with different life cycle inventory techniques, scope, geographical and temporal representations, are used. Compiling life cycle inventories (LCIs) is generally done through three main approaches: process-based analysis (e.g. the approach used in the ICE), input-ouput analysis (originally an economic method which looks at sectoral transactions between the different sectors of an economy), and hybrid analysis (a combination of the previous two). While process-analysis is often credited for better accuracy of specific data linked to the system under examination, it suffers from the so called truncation-error (i.e. neglecting impacts occurring outside the system boundary), and this greatly underestimates requirement [30, 31, 32, 33]. Input-output provides full system coverage, but does so at the expenses of accuracy for it aggregates different sectors within the economy producing average multipliers. Hybrid LCA aims to combine accuracy and system completeness and it has been shown to be likely more accurate than process based LCA [34]. When hybrid analyses have been used to estimate environmental impacts associated with whole buildings, results have shown embodied energy figures up to four times higher than those obtained through process-based LCA [35, 2, 3].

At present, significant improvements and advancements are being made on reliable and transparent databases for the construction sector. For instance, databases such as EPiC (Environmental Performance in Construction) [36] provide embodied GHG coefficients (ECCs) for more than 250 construction materials. Such coefficients express the amount of embodied carbon dioxide equivalent (CO_2e), embodied water and embodied energy per unit mass (or unit volume) of construction material.

1.1. *How much does your structure weigh?*

ECCs represent an essential piece of information in order to assess the environmental impacts of building structures. Assuming the mass values of all the different materials and components making up the structure are known, the overall environmental footprint (e.g. GHG emissions) can then be estimated by first multiplying the relevant coefficient with the mass value of each structural material/component, and then summing up the individual contributions. However, a reliable estimate of the structural masses becomes only available when the design process is well beyond the initial concept stage, i.e. when a series of parameters such as: structural system, geometric layout and materials being used are already specified and only a retrospective assessment can be performed at such point. Moussavi Nadoushani and Akbarnezhad [37] for instance show how design choices related to selection of the structural material (reinforced concrete; steel), building height and type of lateral load resisting system can affect significantly the embodied impacts of building frames.

1.2. Research significance

The current lack of quantitative information, correlating the effect of early-design choices on final structural mass quantities, is clearly limiting the engineers' capability to mitigate the environmental impacts of their designs, with the added risk and tendency to favour some options (e.g. structural material) based on purely *"subjective narrative arguments"* [38], or to simplistically assume a low embodied CO_2 value per unit mass as a sufficient information to prefer one material over the others.

Aim of this study is to facilitate integration of embodied environmental assessment of gravity frame structures in buildings at the early design stage, to enable for an informed comparison (and selection) of alternative design options. The specific objective is therefore to analyse and quantify any existing correlation between material quantities and some basic design parameters such as: bay size of the frame layout, magnitude of floor loads and (main) structural material, namely: reinforced concrete, steel and timber.

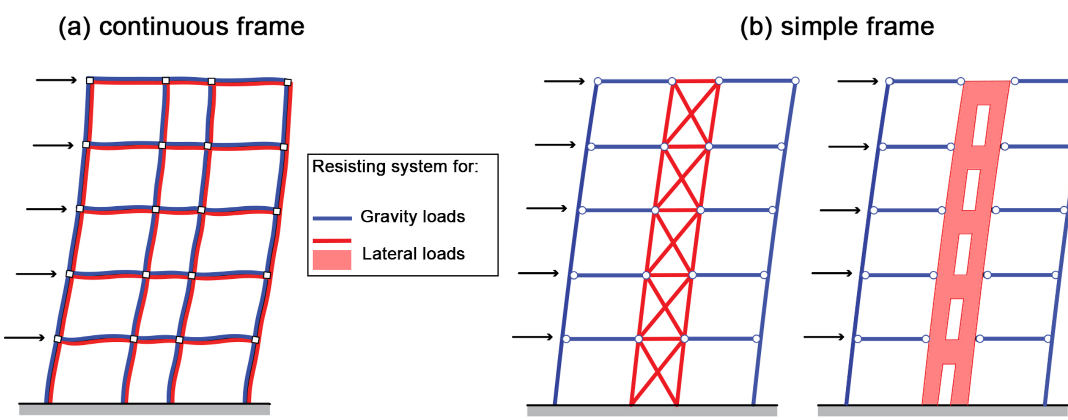

Figure 1: (a) continuous frame—the system of beams and columns resists both vertical and horizontal loads. (b) simple frame—vertical and horizontal loads are resisted by two separate sub-systems.

1.3. Definition of gravity frame system

Before delving in the methodological aspects of this work, an important clarification needs to be made with regard to the definition of gravity frame adopted in here. One of the first choices to make in the preliminary task of designing a building structure is on the selection of a suitable structural system. One of the main parameters dictating the choice for an efficient frame design is usually the building height. According to Fazlur Khan's landmark classification of tall building structural systems [39]: *"...as the building's height increases beyond 10 storeys the lateral sway starts controlling the*

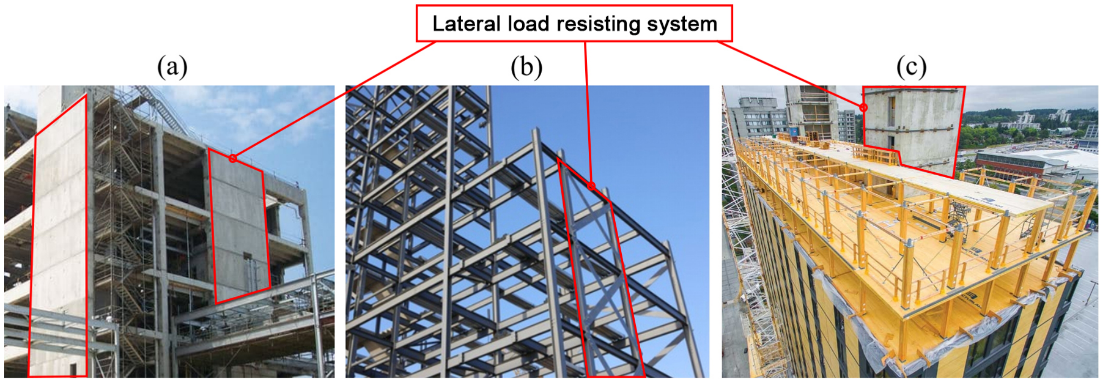

Figure 2: Frame construction according to main structural material: (a) reinforced concrete — image source: [41]; (b) steel — image source: [42]; (c) engineered timber — image source: [43]. The gravity system of beams and columns is coupled with a lateral load resisting system of bracing or shear walls/cores.

design, and stiffness [...] becoming the dominant factor, and the premium for height increases exponentially with the number of stories." [40]. On this basis it can be inferred that for buildings up to 10 storeys (as in our case) lateral stiffness is not a conditioning factor, nonetheless, a requirement for global stability, as well as provision for adequate strength against horizontal actions, would still remain relevant. For low- to mid-rise buildings, the range of suitable options usually boils down to two construction systems: *Continuous* frame, also termed as 'rigid' or 'moment-resisting' frame, and *Simple* frame, also referred to as 'hinged' or 'pinned' frame. One of the differences between the two systems is in the way horizontal loads can be resisted: in continuous frames beam-to-column connections are designed and constructed to act as rigid, therefore allowing the frame to resist vertical loads as well as lateral loads by relying on the bending resistance/stiffness of beams, columns and their mutual connection as shown in Figure 1a. Conversely, in simple frame construction beam-to-column connections are assumed to be nominally pinned, and resistance against lateral loads is provided via a lateral load resisting sub-system (LLRS) such as vertical bracing or shear walls/cores as shown in Figure 2.

We have focused our analysis at the level of the gravity frame sub-system of beams and columns (see Figure 1b)—also termed vertical load resisting system (VLRS)—and thus neglecting the separate mass contribution from the LLRS. While acknowledging that the LLRS can represent a substantial share of the overall structural weight (especially when RC shear walls/cores are used) and thus greatly affecting the overal GHG/energy footprints, we also note that for preliminary members' sizing it is common practice for the VLRS and the LLRS to be *"checked independently"* [44] therefore enabling us to disregard lateral loads in analysing the VLRS system.

2. Methodology

In order to assess the influence of bay size and loads magnitude on structural mass quantities, a stochastic method of analysis is adopted. First, a parametric model of the structural frame is implemented and used to generate a population of several frame design configurations.

2.1. Parametric model

The parametric model is based on a small set of input parameters, described as follows with the help of Figure 3:

- *Geometric parameters*: L_x and L_y indicate respectively the primary and secondary bay spans, while $L_{slab,max}$ is the maximum (allowable) span between secondary beams (it only applies to steel and timber frames). H_{floor} is the inter-storey height.
- *Topological parameters*: n_x and n_y are integers representing respectively the number of bays along the primary and secondary structural grid directions, whereas n_{floor} is the total number of floors (e.g. for the frames shown in Figure 3 we have: $n_x = 3$, $n_y = 2$ and $n_{floor} = 4$).
- *Loading parameters* (characteristic values): q_{floor} and g_{fin} are respectively the imposed (variable) floor load and the permanent floor load due to floor finishes, ceiling, services and partitions, whereas g_{env} is the line-load (e.g. in kN/m) due to the building's cladding and envelope walls.

An initial population of design configurations was generated by randomly picking values for each (geometric, topological and loading) input parameter from within a given interval. Lower and upper bound values for each parameter's interval are summarised in Table 1. Design configurations whose footprint area ($= L_x n_x L_y n_y$) exceeded 5'000 m^2 were discharged, eventually obtaining a total of 10'460 valid frame designs. A constant value for $L_{slab,max} = 2.6$m was considered for all (steel and timber frame) configurations. The number of secondary beams between each primary bay ($n_{s,b}$)[1], was taken as the

[1] i.e. $n_{s,b} = 2$ for the steel and timber frame configurations shown in Figure 3.

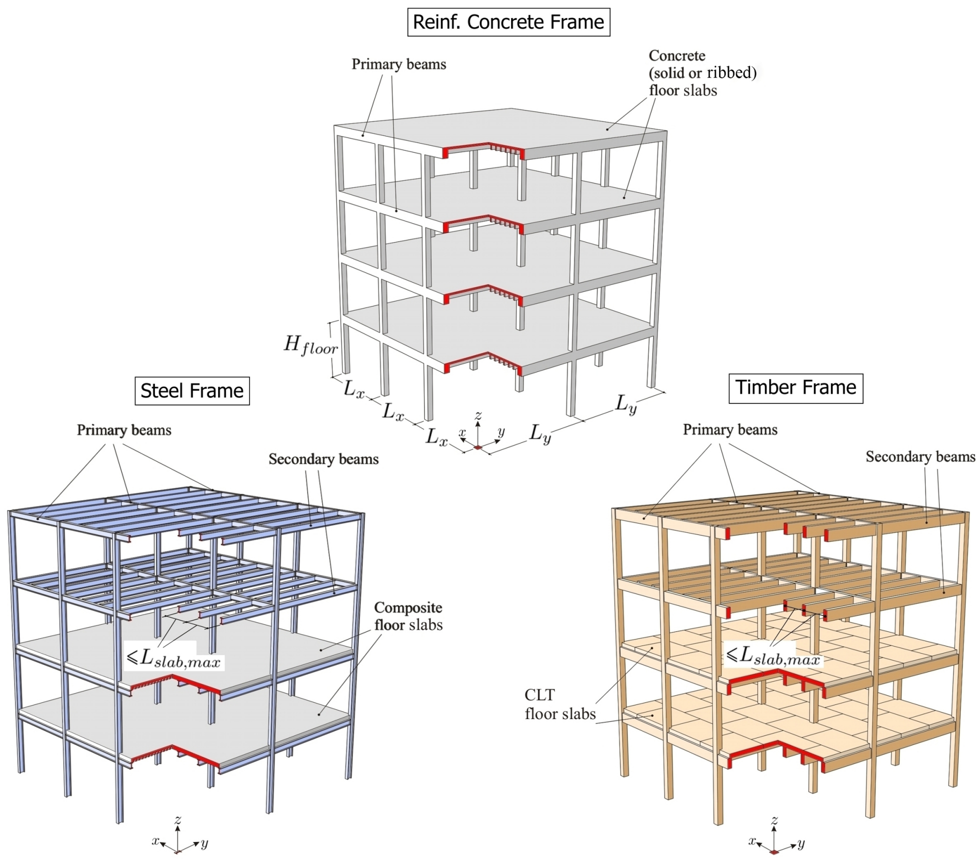

Figure 3: Terms and symbols to indicate the geometric and topological parameters of the structural frame model.

smallest integer such that—given a certain primary bay's length L_x—the floor slabs spanning along the x direction do not exceed the allowable $L_{slab,max}$ value [45]:

$$n_{s,b} = max\left\{0\ ;\ ceiling\left(\frac{L_x - L_{slab,max}}{L_{slab,max}}\right)\right\} \tag{1}$$

For a given argument x, the *ceiling()* function in Eq. 1 returns the smallest integer $\geq x$.

Secondary beams in-between primary bays are only considered for steel and timber frames, as reinforced concrete (RC) frames were assumed to have (one-way) floor slabs directly supported by primary beams. Therefore no secondary beams were accounted for in the RC parametric model, except at the edges where it is assumed that secondary beams are required to carry the line-load due to the building's envelope walls and cladding. The three material options were then assigned to each of the 10'460 design configuration so generated, thus obtaining a total of 31'380 different frame design data points. It is also worth pointing out that each of the three material options being considered includes a combination of structural materials (see Figure 3). Specifically:

- *Reinforced concrete frame*: a combination of concrete and reinforcement steel.
- *Steel frame*: hot rolled steel profiles (for beams and columns) and cold rolled steel sheeting and concrete (for the composite floor slabs).
- *Timber frame*: glue laminated timber (glulam) members for beams and columns, and cross laminated timber (CLT) panels for the floor slabs.

Table 1: Lower and upper bound parameter values used to generate a population of design frame data points.

Parameter	Unit	Lower bound value	Upper bound value
L_x	m	5.0	8.5
L_y	m	L_x	12.0
H_{floor}	m	3.5	4.0
n_x	No	1	20
n_y	No	1	20
n_{floor}	No	1	10
q_{floor}	kN/m^2	1.5[a]	5.0[a]
g_{fin}	kN/m^2	0.0	0.6
g_{env}	kN/m	2.0[b]	12.0[c]

[a]Based on Categories of loaded area A, B and D as from BS EN 1991-1-4 [46].

[b]For lightweight steel infill walls.

[c]For concrete infill walls.

2.2. Computing structural masses

In order to automate the task of evaluating structural masses for the entire population of 31'380 design data points, a set of computer algorithms were specifically developed in IronPython programming language [47] combined with Math.NET Numerics library [48] to analyse, optimise and rationalise all structural member sections. Indeed, frame masses can be straightforwardly derived once the volumes of structural elements are known, and since member lengths and floor slab surface-areas are readily available (as geometric input parameters), the remaining unknowns required to estimate the structural volumes are the members (beams and columns) sectional areas and floor slab thicknesses.

2.2.1. Structural analyses

Given the geometric and topological input parameter values it is possible to build a 3-dimensional model of the structural frame in terms of list of nodal coordinates and connectivity-list (i.e. the way members are connetted to each other) [45]. Then, based on the design values of the input loading parameters[2], structural analyses of the entire frame are performed via Direct Stiffness Method (DSM) [50], therefore obtaining the internal forces, moments and deflections for each member. The DSM implementation requires preliminary computation of stiffness matrices for each (beam and column) element which are computed from the list of nodal coordinates and eventually assembled into a global stiffness matrix. Support restraints and applied external forces (loads) are then added to the global system of stiffness equations, therefore enabling for automatic identification and extraction of a sub-system of linear equations:

$$\mathbf{f} = \mathbf{K}\mathbf{x} \tag{2}$$

with $\mathbf{f}$ being the vector-list of applied nodal loads; $\mathbf{x}$ is the corresponding vector-list of unknown nodal displacements and $\mathbf{K}$ is a square stiffness matrix with row (and column) size $= 3(n_x + 1)(n_y + 1)n_{floor}$ in our specific case. For each load combination the linear system in Eq. (2) is solved for $\mathbf{x}$ therefore obtaining the nodal displacements (and hence the internal deformations and forces) of each element.

In addition to input-defined permanent and variable loads, the permanent loads due to the structure's self-weight are automatically computed based on assigned values of material densities. Nominally pinned connections are assumed for the frame models as being more commonly used in construction than rigid or semi-rigid ones due to the lower fabrication costs. We note that assuming nominally pinned connections yields to more conservative design for the members' cross-section than assuming rigid or semi-rigid connections. This because critical parameters such as maximum bending moment and/or maximum deflection, are higher in the former case.

2.2.2. Sizing beams and columns

For a given set of input parameter values, structural analyses are iteratively performed as part of an optimisation routine, employed to minimise the cross-section of structural members against a set of (optimisation) constraints. Such constraints are

[2]Design load values are obtained by multyplying the characteristic input values (and self-weights) with the appropiate partial safety factors as per BS EN 1990:2002 requirements [49].

introduced to account for a series of Eurocode-based design requirements at both Serviceability and Ultimate Limit States [51, 52, 53] for the individual beam or column in terms of resistance, stability and deflection limits. Specifically, the optimisation method enables to find the minimum cross-sectional area of primary and secondary beams such that design requirements for bending resistance, lateral torsional buckling, shear and deflection are all satisfied, as well as to find the minimum cross-sectional area of columns against the requirements for compressive resistance and axial buckling.

The optimisation method relies on a Sequential Search (SS) algorithm [54] to seek the optimal cross-section from within a finite set of available profiles. For Steel frames, such finite set is based on the Blue Book catalogue, limitedly to Universal Beam and Universal Column sections [55]. For RC and glulam members, the sequential search is instead performed on a range of square and down-stand rectangular sections (at size increments of 1cm) for columns and beams respectively. Overall masses of steel reinforcement are estimated ex post, as a percentage of the concrete mass, specifically: 12.5% for columns, 10.5% for beams and 8.5% for floor slabs. The percentage values are based on practitioners' estimates [56].

The implemented structural analysis and optimisation methods briefly described in sections 2.2.1 and 2.2.2 are an extended version (to timber and RC frames) of the set of methods described in [45], originally developed by the authors for steel frames only. We encourage the interested reader to refer to [45] for an in-depth description of these methods.

To take into account the influence of design rationalisation on structural masses, the optimised cross-sections are rounded-off into groups: a uniform cross-sectional area is assumed for all columns that are vertically aligned, taken as the biggest area section within that line of columns. Similarly, two cross-section designations are considered within each floor, one for primary beams and one for secondary beams.

2.2.3. Floor slabs

All floor slabs in steel and timber frames are supported by secondary beams spaced at a distance always close to, and smaller than, $L_{slab,max} = 2.6$ m (see Eq. 1). Therefore it is reasonable to assume constant mass values per unit area for both types of slab. For composite floor, used in steel frame construction, it is assumed a steel deck sheet with a mass per unit area of 11.5 kg/m^2 and a concrete filling weighting 260 kg/m^2 [57]. CLT panels with a mass of 45.6 kg/m^2 are considered instead for timber frames, the value is estimated based on a panel depth of 100 mm. Due to the high variability in span lengths

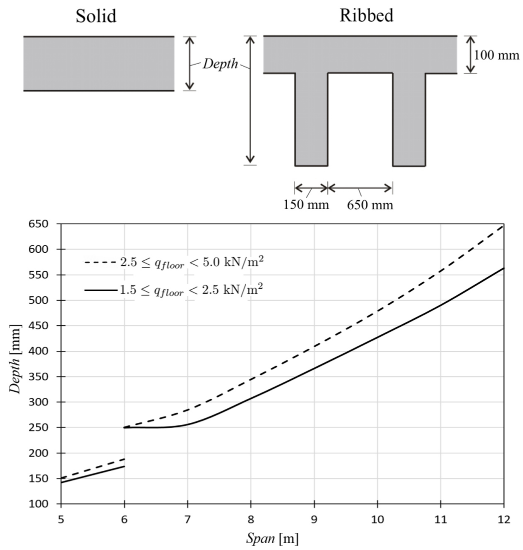

Figure 4: Depth of (one-way) RC floor slabs as a function of span and imposed load, adapted from [44].

of cast-in-situ RC floor slabs, $\in$ [5m; 12m], functions expressing the span-to-depth ratio are adopted from [44] in order to derive mass values of RC floors per unit area. Such functions are shown in Figure 4: as it can be seen, a distinction is made between RC floors spanning up to 6m, for which a *solid* slab is assumed, and RC floors with a span above 6 m for which *ribbed* slabs are considered instead.

2.2.4. Material properties

Steel grade S275 is assumed for the hot rolled (beam and columns) profiles, whereas C35 concrete and reinforcement steel with a yield strength of 460 N/mm^2 is considered for the RC frames. A Strength Class GL24h is instead assumed for all glulam members. Mesh reinforcement and shear studs in composite floor slabs were not included in the steel mass calculation.

2.3. Model assumptions and limitations

A limitation of the work presented herein is the very specific and limited combination of commercially available construction products/systems for the three frames for each material option. For instance, a wealth of alternative pre-cast products exist for RC floor slabs which could be used in both RC frames as well as steel frames. Similarly, we limited the selection of steel sections to Universal Beams and Columns [55] whereas Castellated and Cellular sections may be considered in practice.

A further limitation of the study (already introduced in section 1.3) is that our analysis is limited to the VLRS, therefore excluding the mass contribution of the LLRS. We do so based on the assumption that horizontal loads are entirely resisted by the LLRS, therefore allowing us to only consider the effect of vertical loads on the VLRS. Given however that in some cases it is not possible to completely isolate the two structural sub-systems [58], the error deriving from such assumption—of neglecting any effect of lateral loads on the VLRS—is preliminary checked via sensitivity analysis.

2.3.1. Sensitivity analysis

From the population of generated frame models we select a tall, slender geometry within the *Steel frame* sample group and include a LLRS of cross-bracing to the VLRS model (as shown in Figure 5) therefore we consider additional load combinations during analysis accounting for lateral load cases in addition to gravity loads. The obtained steel mass of the VLRS (i.e. excluding steel cross-bracing) is then compared to the one previously obtained without accounting for lateral wind loads, hence allowing us to quantify the assumption error.

The additional lateral load cases considered during analysis are taken as representative of the wind pressure acting on the building's envelope for the full 360° range of directions, as explained in Ref. [45]. A charachteristic value of 1.50 kN/m^2 is considered for the wind pressure loads, calculated according to Eurocode procedures [59, 60] with Glasgow urban area assumed as the building location—for it being in a high wind speed region compared to the rest of the UK.[3] The horizontal deflection limit for inter-storey drift set for analyses ($\leq H_{floor}/300$) is taken in accordance with UK Natioanl Annex to Eurocode 3 [61].

The analysis model excluding wind loads gives an overall steel mass of 262.3 t for the VLRS. This figure increases to 280.1 t when accounting for the model including wind loads, corresponding to an error underestimate of circa 6%. The structural elements of the VLRS experiencing highest error in terms of mass-underestimation are the columns nearby the corners. This is somehow expected given these are the columns connected to the system of bracing[4] as shown in Figure 5 and therefore, in addition to bearing gravity loads, these columns also resist additional axial forces resulting from the LLRS cantilever effect required to resist the horizontal wind loads.

[3]See UK map of fundamental basic wind velocity [60].

[4]These columns are effectively an integral part of the LLRS.

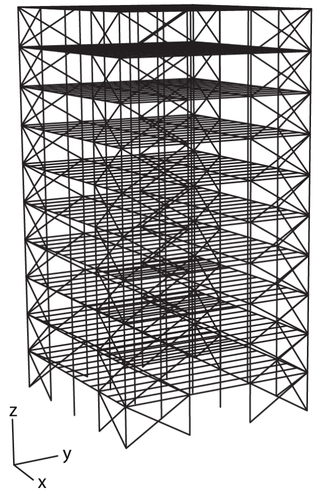

Figure 5: Steel frame geometry used for sensitivity analysis ($L_x = 5.40$ m; $L_y = 6.65$ m; $H_{floor} = 3.9$ m; $n_x = 4$; $n_y = 3$; ; $n_{floor} = 10$). The LLRS comprises cross-bracing placed at the four corners of the frame layout plan.

3. Results and discussions

The structural masses of each design frame data point have been normalised to the corresponding gross floor area ($= L_x n_x L_y n_y n_{floor}$) thus obtaining mass values per square metre of floor area for each material option (i.e. RC, steel and timber). Such mass quantities are shown in Figure 6, with boxes indicating the interquartile range around the median (bolt line), and whiskers indicating the 5% to 95% range. As mentioned previously, the amounts of steel and concrete for the composite floor deck, as well as for CLT floor slabs, are assumed to be constant and thus no variation ranges are shown in Figure 6 for them.

Table 2: Aggregated mass quantities per unit floor area. Values disaggregated per structural component are shown in Figure 6.

	RC frame	steel frame	timber frame
This study[a] [kg/m^2]	465	345	90
De Wolf et al. [kg/m^2]	1090	845	203
This study [normalised]	5.2	3.8	1.0
De Wolf et al. [normalised]	5.3	4.1	1.0

[a]Mass quantities associated with shear walls/cores, and substructure are not included in this study.

The values[5] of mass quantities for each material option (RC, steel, timber) have

[5]Mean values were considered for concrete, steel (reinf. rebars), steel (hot rolled profiles) and timber

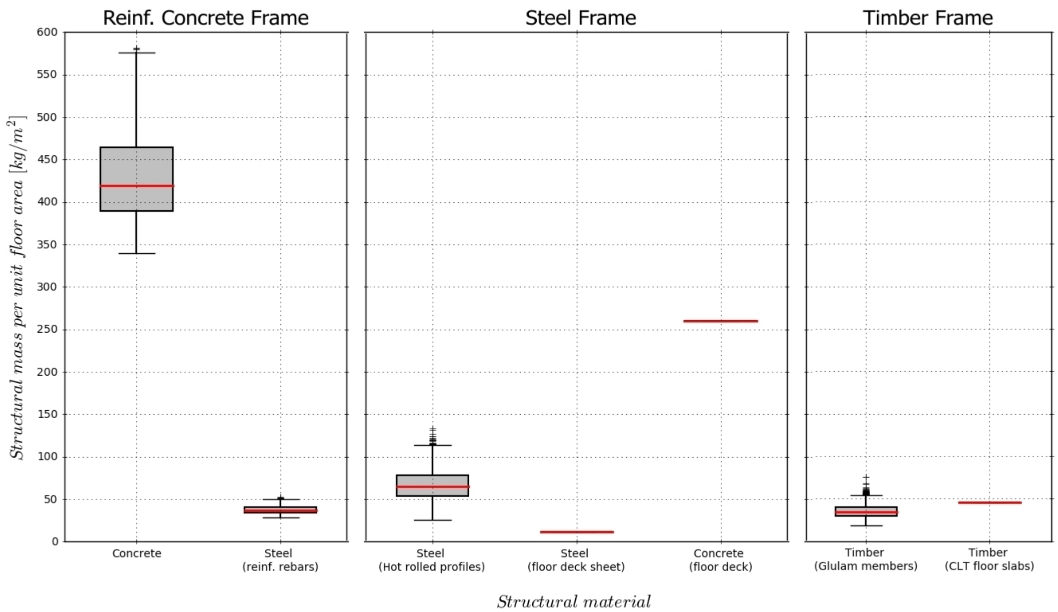

Figure 6: Mass quantities per unit floor area. Median values indicated with bolt line.

been summed up and reported in Table 2, along with the mass quantities given in De Wolf et al. [23]. These latter values were collected from industry, based on a number of real project case studies. Both sets of values have been normalised to the mass value of timber frames and are also shown in Table 2. It can be seen from the Table that mass quantities per square metre provided by De Wolf et al. are roughly double of those found in here. This is easily explained by reminding that our analysis has been limited to the VLRS only (i.e. excluding shear walls/cores, foundations and any other substructure component). Nonetheless, when looking at the normalised values they look remarkably similar, suggesting that assessing only the VLRS (beams, columns and floor slabs) can actually be a proxy for a broader system boundary of the assessment, for the trends are nearly identical.

3.1. Regression analyses: least squares

3.1.1. Influence of bay area

For completeness, histograms of the mass quantities for concrete (excluding reinforcement rebars), steel and timber beams and columns (i.e. hot rolled profiles and glulam members, respectively) are also shown, in Figure 7. In order to analyse any existing

(CLT floor slabs).

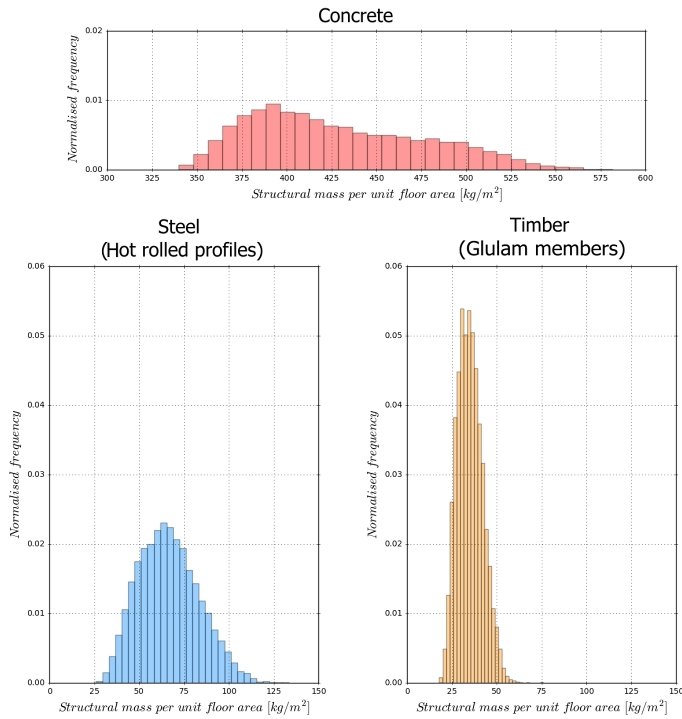

Figure 7: Histograms of structural mass quantities for RC frames (included floor slabs), steel and timber frames (beams and columns only). See Figure 6 for reference.

correlation between the mass quantities and variations of the frame geometry—namely, the bay area ($a = L_x L_y$)—linear and exponential functions are fitted via least square regression [62]. The results are shown in Figure 8. Before discussing the findings shown in Figure 8 it is worth noting that it would be inconsistent to directly compare the average (concrete, steel and timber) mass quantities for a given bay area a. In fact, the graph on the left side of the Figure provides values of concrete masses (excluded reinforcement) for the RC frame including the masses of floor slabs, whereas floor slab masses are not included in the two graphs on the right (i.e. for steel and timber). This happens because their mass amounts per unit floor area are both assumed to be constant, as explained in section 2.2.3 and shown on Figure 6, and thus uncorrelated to the bay size a. A comparison in terms of increment of mass per unit floor area among the three material options (i.e. only in terms of slope coefficients C_1 for the linear function $m = C_1 a + C_2$) is certainly legit. With reference to Figure 8, we found that for 1 m^2 increase of the bay area an additional 0.26 kg/m^2 of glulam is required on average. This latter figure is about 0.84 kg/m^2 when hot rolled steel profiles are used instead. Two distinct trends can be observed for RC frames, depending on the type of floor slab

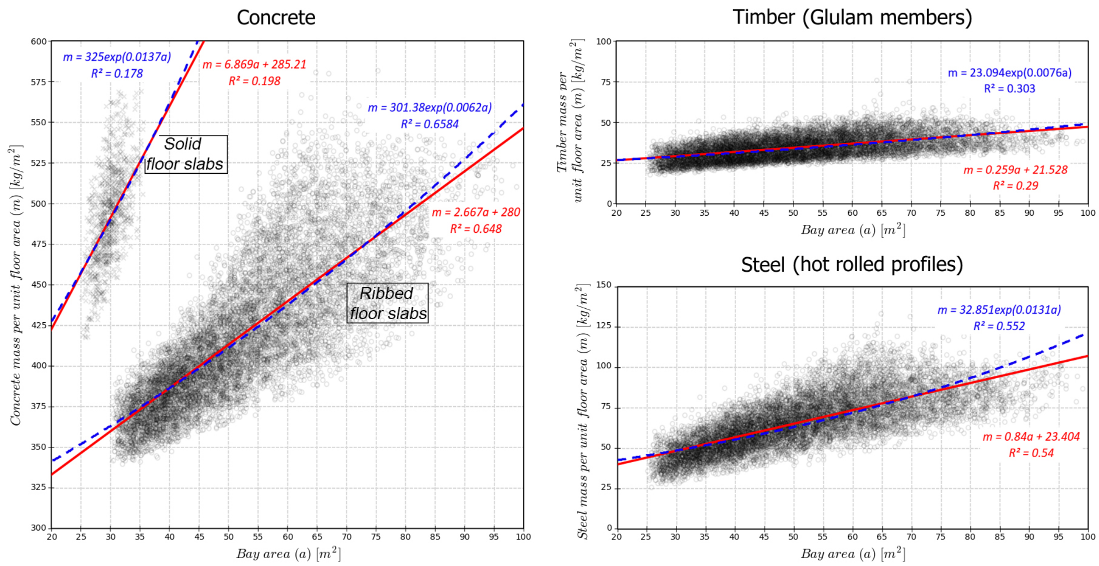

Figure 8: Least squares regressions of bay areas (a) vs. mass quantities (m) for RC frames (included floor slabs), steel and timber frames (beams and columns only). Two functions are considered for fitting: a linear function, $m = C_1a + C_2$ (continuous line) and an exponential function, $m = C_1e^{C_2a}$ (dashed line).

construction being used (solid or ribbed). In the first case an heavier frame is obtained, requiring circa 6.87 kg/m^2 of (plain) concrete for every 1 m^2 increase of the bay area, whereas for ribbed slabs the increase per unit mass is much lower ($\approx$ 2.67 kg/m^2).

3.1.2. Influence of floor loads

As for the bay area, structural masses are indeed also influenced by the magnitude of floor loads that the frame is required to carry. Such a correlation between structural masses (m) and magnitude of floor loads ($p = q_{floor} + g_{fin}$, i.e. excluded self-weight), as well as bay area (a), can be visualised in Figure 9, in which the population of design frame data points, previously shown in Figure 8, has been extended to the third dimension, p, for all three material options.

A linear least squares regression analysis is performed for each of the three material options. Numerical values of the coefficients C_1, C_2 and C_3 for the fitting plane Equations $m = C_1a + C_2p + C_3$ are also provided in Figure 9, along with the corresponding R^2 values.

By comparing R^2 values in Figure 8 with those of the linear function in Figure 9 it is clear that a better fit is achieved when both (bay area and magnitude of floor loads) parameters are considered as independent variables instead of bay area only. Specifically, for 1 kN/m^2 floor load increase an additional 4.13 kg/m^2 of glulam ($\approx$ 5 kg/m^2 of hot

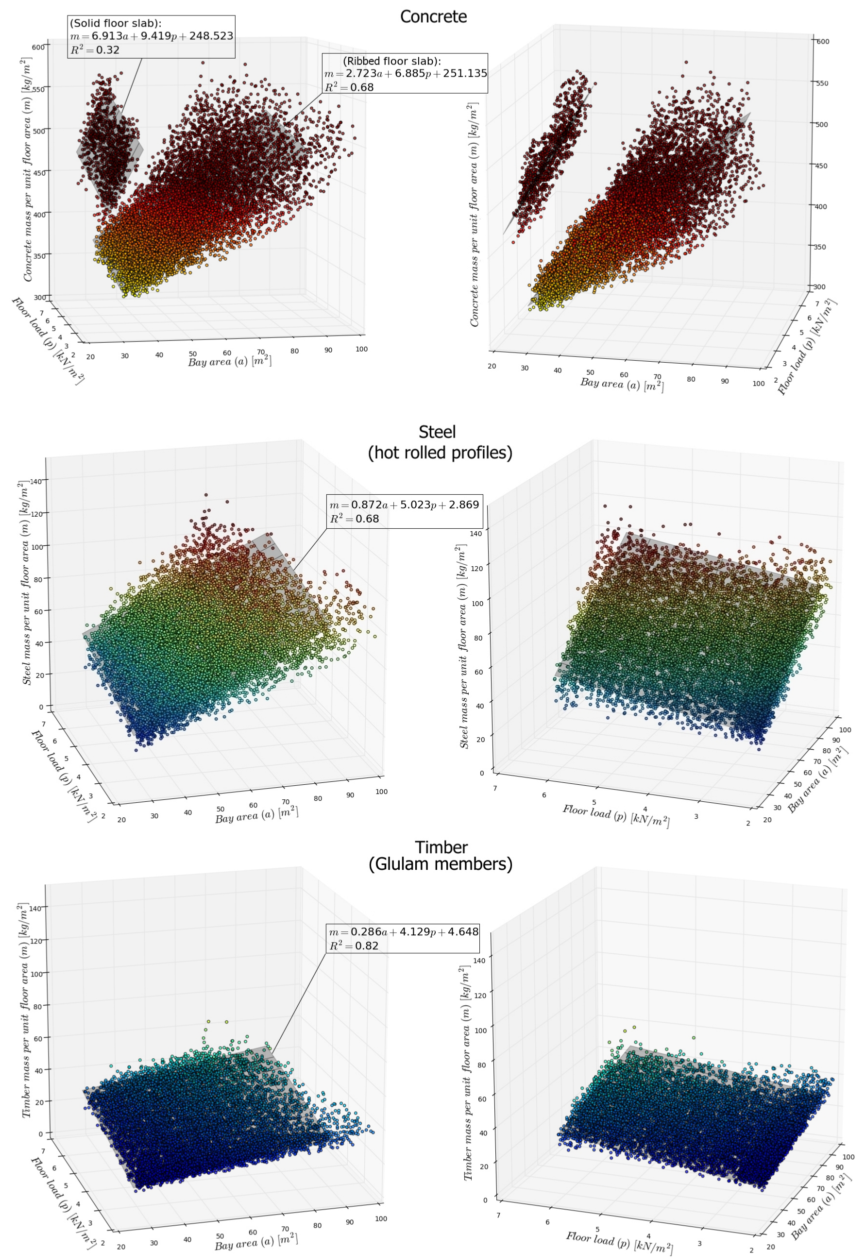

Figure 9: Least squares regression of bay areas (a) and floor loads ($p = q_{floor} + g_{fin}$) vs. mass quantities (m) for RC frames (included floor slabs), steel and timber frames (beams and columns only). The linear function $m = C_1 a + C_2 p + C_3$ is used for fitting.

rolled steel) is required on average. When solid slabs are used in RC frames, a 1 kN/m^2 increase of the floor loads results in an average 9.4 kg/m^2 of additional concrete. The same figure is reduced to 6.9 kg/m^2 when ribbed slabs are used instead.

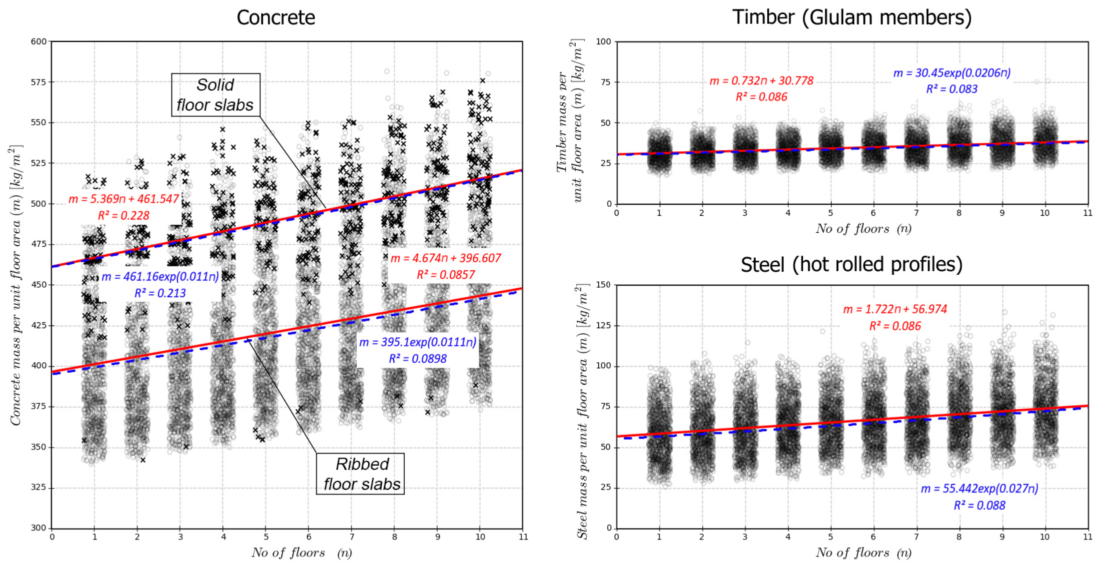

Figure 10: Least squares regression of No of floors (n) vs. mass quantities (m) for RC frames (included floor slabs), steel and timber frames (beams and columns only). Two functions are considered for fitting: a linear function, $m = C_1 n + C_2$ (continuous line) and an exponential function, $m = C_1 e^{C_2 n}$ (dashed line).

3.1.3. Influence of floor number

For the sake of completeness, plots showing the normalised mass quantities against the number of floors is also shown in Figure 10. Expectedly, structural masses of the frames increase with the increase of the number of floors for all three material options. It should be reminded however that such correlations do not take into account the effect of lateral loading on the mass of both VLRS and LLRS which would increase exponentially with building's height according to Khan's analysis [39].

3.2. Regression analyses: quantile regression

In the previous section, linear least squares regressions have been applied to the sample population of (numerically generated) design frame data points in order to assess the influence of bay area (a), floor load magnitude (p) and number of floors (n) on the dependent variable m, that is to say, the structural mass per unit of floor area.

As shown in Figures 8 and 10, both linear and exponential functions yield very similar coefficients of determination. Low R^2 values indicate a high degree of variability (scatter) of the dependent variable m around the regression curves, meaning that such regression curves would perform poorly for the task of predicting single observations. Nonetheless, the data points shown in Figures 8 and 10 have been fitted for the sole purpose of showing the *statistical* trend between independent and dependent variables.

Clearly, the existence of such trend is unaffected by the variability of m_i data points around the fitted curve.

Although insightful, the found correlations only provide information limited to the average trends of the sample population. From a practical point of view, it may be more useful for the structural designer to be informed on the degree of variability associated to m (which we know is quite high given the low R^2 values), ideally in terms of minimum and maximum probability ranges, and also to know the extent to which such ranges change as a function of the independent variables a and p. Quantile regression [63] is employed for this purpose. The main difference between the two methods (least squares and quantile regression) is briefly explained as follows. Given a predictor function $f(a) = C_1 a + C_2$, the least squares method consists of finding optimal values for the two coefficients (C_1, C_2) such that the sum of squared residuals is minimised:

$$min: \quad \sum_{i=1}^{n} \left[m_i - f\left(a_i\right)\right]^2 \tag{3}$$

with m_i and a_i being respectively the structural mass per unit floor area and bay area of the ith data point respectively, and n is the total number of design frame data points for a given material (i.e. $n = 10460$ in our case). In quantile regression, the loss function being minimised is instead defined as follows:

$$min: \quad \sum_{i=1}^{n} \rho_\tau |m_i - f\left(a_i\right)| \tag{4}$$

where:

$$\begin{cases} \rho_\tau = \tau & \text{for } m_i \geq f\left(a_i\right) \\ \rho_\tau = (1-\tau) & \text{for } m_i \leq f\left(a_i\right) \end{cases} \tag{5}$$

and with $\tau \in [0; 1]$ indicating the probability quantile of interest. For instance, by setting $\tau = 0.5$ would yield the regression line $f(a)$ to approximate the *median* quantile.

Quantile regression analyses have therefore been applied to the sample populations of structural masses previously shown in Figure 8, assuming 5% and 95% quantiles (i.e. $\tau = 0.05$ and 0.95 respectively) except for concrete masses of RC frames with solid floor slabs, for which a single (median) quantile value is considered. Lines of best fit are shown in Figure 11. As it can be seen, for each of the three material options there are eight linear fits: four lines fitting the 5% quantile and four more for the 95% quantile. This because the entire populations of three material options, have been 'sliced' into four sub-sets according to the floor loads variable p. Limit values of floor loads, defining the boundaries of the four sub-sets, are taken at constant increments of 1 kN/m^2, starting from 2 kN/m^2 up to 6 kN/m^2.

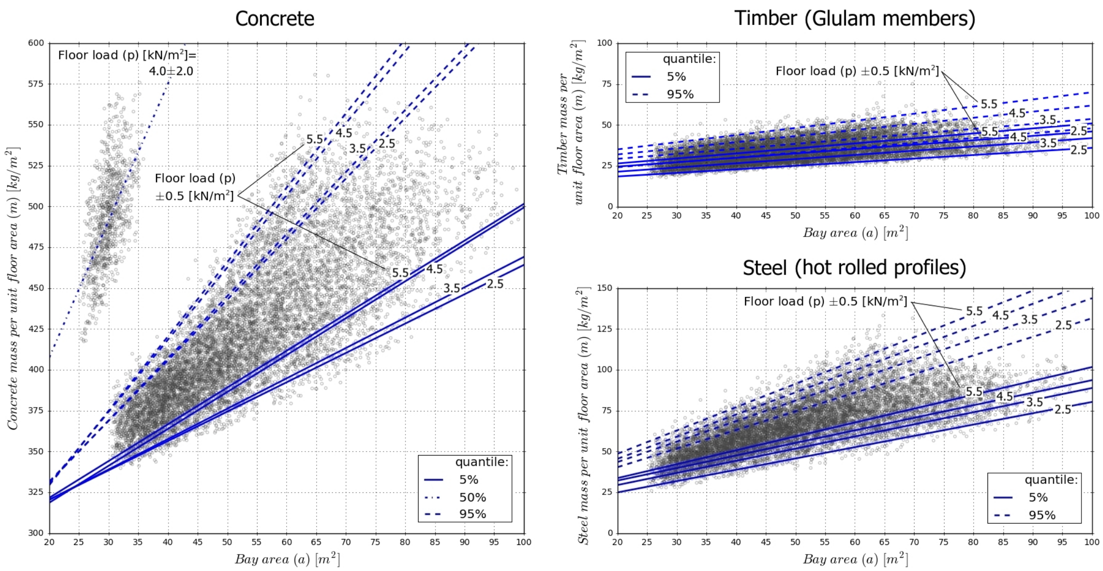

Figure 11: Quantile regression of bay areas (a) vs. mass quantities (m) for RC frames (included floor slabs), steel and timber frames (beams and columns only). See Figure 6 for reference.

To facilitate readings of the prediction ranges shown in Figure 11, the values of regression coefficients C_1 and C_2 have been summarised in Table 3. Accordingly, for a given material option and magnitude of floor loads p, minimum and maximum values of structural mass m are easily obtained by setting the corresponding slope and intercept values (as from Table 3) in the linear Equation $m = C_1 a + C_2$.

We believe that the Table of coefficients provided in here can be of practical and immediate use at preliminary stages of the structural design, which is when the plan layout of building frames is first laid down, and thus an average size of bay areas is also defined. Accordingly, predictions of the structural masses (along with their uncertainty range) and consecutive GHG/energy intensities can be straightforwardly obtained.

4. Discussion and conclusions

Structures are largely responsible for the material and resource intensity of buildings over their whole life cycle. Therefore, knowing a priori the amount of structural material used can prove significantly beneficial for reducing the embodied environmental flow of structural systems for buildings. This paper has addressed the issue from an early stage design perspective (limitedly to gravity frames) when change is most feasible and less

Table 3: Regression coefficients to predict the minimum and maximum values of structural mass $m = C_1 a + C_2$ as a function of: main structural material, magnitude of floor load (p) and bay area (a). A graphical representation of the regression lines is shown in Figure 11.

Material option	Floor load[a] (p) [kN/m^2]	Quantile [%]	Regression coefficients: Slope (C_1)	Regression coefficients: Intercept (C_2)
concrete (ribbed floor slabs)	2.5 ± 0.5	5	1.796	284.628
		95	3.708	257.553
	3.5 ± 0.5	5	1.858	283.297
		95	3.801	255.033
	4.5 ± 0.5	5	2.258	273.557
		95	4.414	241.916
	5.5 ± 0.5	5	2.249	276.740
		95	4.551	238.470
concrete (solid floor slabs)	4.0 ± 2.0	50	8.381	239.945
steel[b] (hot rolled profiles)	2.5 ± 0.5	5	0.692	11.148
		95	1.140	17.639
	3.5 ± 0.5	5	0.742	14.669
		95	1.254	18.501
	4.5 ± 0.5	5	0.768	16.872
		95	1.355	18.457
	5.5 ± 0.5	5	0.850	16.766
		95	1.426	20.121
timber[b] (glulam members)	2.5 ± 0.5	5	0.219	14.120
		95	0.298	18.199
	3.5 ± 0.5	5	0.257	16.300
		95	0.305	23.195
	4.5 ± 0.5	5	0.268	19.203
		95	0.374	24.508
	5.5 ± 0.5	5	0.306	20.353
		95	0.437	26.372

[a] p = (characteristic) variable floor load plus permanent load due to finishes, ceiling, services and partitions.

[b] Mass of beams and columns only, i.e. mass of floor slabs is not accounted.

costly. he t Early stage design is characterised by little and imperfect information about the final details of a building structure and for this reason a parametric approach based on very few input parameters was used. A large population (31'180 samples) of realistic building frames formed the primary data for the analysis across three main structural typologies: reinforced concrete, steel, and engineered timber.

Results show that the resource intensity is lowest in the case of engineered timber and highest for reinforced concrete, with steel in between. However, in the case of steel, the greatest component of its overall mass comes from the concrete floor slabs. If the analysis were limited to the bare frames only (i.e. exuding floor slabs), steel and timber would be somewhat within comparable ranges. This suggests that a greater efficiency in steel-framed structures could be achieved by using lighter alternatives to cast-in-situ concrete floor slabs. The range of existing products and their combined use in the construction of building frames is extremely wide and not fully accounted for in here. We have limited the analysis to a particular combination of material/construction technologies when defining the three material options. Furthermore, the study was limited to the vertical load resisting frame system only, hence excluding the additional mass contribution form the lateral load resisting system, as well as any ground work foundation. We stress all the aforementioned limitations should be taken into account when using the findings presented herein.

Findings have been compared with previous works based on industry-data from other geographical areas. The comparison suggests that assessing the VLRS only (as in this paper) can be a proxy, at least early in the design stage, for more time-consuming analyses which would include the lateral load resisting system (bracing, shear walls/cores) and foundations. Normalised results related to material intensity per unit of floor area are also remarkably close to industry-based data, suggesting that the proposed approach indeed identifies numbers that do match what then happens in the reality of construction projects.

Results have been statistically analysed through least squares and quantile regression techniques. Such analyses allowed to obtain strongly correlated equations to link the structural mass of the frame system to merely three inputs: structural material, bay area and floor load. This finding can be particularly useful at early stages of the design process for they allow to easily 'weigh' the structural frame option and test several alternatives in a short time and with little effort. Future research could extend the present work to link masses with environmental impacts across a number of categories (e.g. embodied energy, GHGs emissions, resource depletion).

5. Acknowledgements

The research work presented in here is supported by the UK's Engineering and Physical Sciences Research Council (EPSRC) [Grant No. EP/R01468X/1]. We also gratefully acknowledge Bengt Cousins-Jenvey and Clement Thirion from Expedition Engineering for their valuable comments on this paper. Acknowledgements are finally extended to the anonymous reviewers whose comments, we feel, have greatly improved the final version of the paper.

References

[1] T. Abergel, B. Dean, J. Dulac, Towards a zero-emission, efficient, and resilient buildings and construction sector: Global status report 2017, UN Environment and International Energy Agency: Paris, France.

[2] R. H. Crawford, A. Stephan, The significance of embodied energy in certified passive houses, in: Proceedings of World Academy of Science, Engineering and Technology, no. 78, World Academy of Science, Engineering and Technology (WASET), 2013, p. 453.

[3] A. Stephan, L. Stephan, Reducing the total life cycle energy demand of recent residential buildings in lebanon, Energy 74 (2014) 618–637.

[4] R. Rovers, Zero-energy and beyond: A paradigm shift in assessment, Buildings 5 (1) (2014) 1–13.

[5] F. Pomponi, A. Moncaster, Scrutinising embodied carbon in buildings: The next performance gap made manifest, Renewable and Sustainable Energy Reviews, (2017).

[6] A. Dimoudi, C. Tompa, Energy and environmental indicators related to construction of office buildings, Resources, Conservation and Recycling 53 (1-2) (2008) 86–95.

[7] S. Kaethner, J. Burridge, Embodied co2 of structural frames, The structural engineer 90 (5) (2012) 33–40.

[8] J. M. Allwood, M. F. Ashby, T. G. Gutowski, E. Worrell, Material efficiency: A white paper, Resources, Conservation and Recycling 55 (3) (2011) 362–381.

[9] A. Liew, D. L. López, T. Van Mele, P. Block, Design, fabrication and testing of a prototype, thin-vaulted, unreinforced concrete floor, Engineering Structures 137 (2017) 323–335.

[10] W. Hawkins, J. Orr, P. Shepherd, T. Ibell, Design, construction and testing of a low carbon thin-shell concrete flooring system, in: Structures, Elsevier, 2018.

[11] A. Bukauskas, P. Shepherd, P. Walker, B. Sharma, J. Bregulla, Inventory-constrained structural design: New objectives and optimization techniques, in: Proceedings of IASS Annual Symposium, International Association for Shell and Spatial Structures (IASS), 2018.

[12] J. Brütting, J. Desruelle, G. Senatore, C. Fivet, Design of truss structures through reuse, in: Structures, Vol. 18, Elsevier, 2019, pp. 128–137.

[13] C. F. Dunant, M. P. Drewniok, S. Eleftheriadis, J. M. Cullen, J. M. Allwood, Regularity and optimisation practice in steel structural frames in real design cases, Resources, Conservation and Recycling 134 (2018) 294–302.

[14] J. Orr, M. Drewniok, I. Walker, T. Ibell, A. Copping, S. Emmittc, Minimising energy in construction: Practitioners' views on material efficiency, Resources, Conservation and Recycling 140 (2019) 125–136.

[15] M. C. Moynihan, J. M. Allwood, Utilization of structural steel in buildings, Proc. R. Soc. A 470 (2168) (2014) 20140170.

[16] A. D. Lee, P. Shepherd, M. C. Evernden, D. Metcalfe, Optimizing the architectural layouts and technical specifications of curtain walls to minimize use of aluminium, Structures 13 (2018) 8–25.

[17] B. D'Amico, F. Pomponi, Sustainability tool to optimise material quantities of steel in the construction industry, Procedia CIRP 69 (2018) 184–188.

[18] T. Ramesh, R. Prakash, K. Shukla, Life cycle energy analysis of buildings: An overview, Energy and buildings 42 (10) (2010) 1592–1600.

[19] F. Pomponi, A. Moncaster, Embodied carbon mitigation and reduction in the built environment–What does the evidence say?, Journal of environmental management 181 (2016) 687–700.

[20] C. De Wolf, F. Pomponi, A. Moncaster, Measuring embodied carbon dioxide equivalent of buildings: A review and critique of current industry practice, Energy and Buildings 140 (2017) 68–80.

[21] L. Vukotic, R. Fenner, K. Symons, Assessing embodied energy of building structural elements, Proceedings of the Institution of Civil Engineers – Engineering Sustainability 163 (3) (2010) 147–158.

[22] P. Foraboschi, M. Mercanzin, D. Trabucco, Sustainable structural design of tall buildings based on embodied energy, Energy and Buildings 68 (Part A) (2014) 254–269.

[23] C. De Wolf, F. Yang, D. Cox, A. Charlson, A. S. Hattan, J. Ochsendorf, Material quantities and embodied carbon dioxide in structures, Proceedings of the Institution of Civil Engineers – Engineering Sustainability 169 (4) (2016) 150–161.

[24] J. Helal, A. Stephan, R. Crawford, Towards a design framework for the structural systems of tall buildings that considers embodied greenhouse gas emissions, in: Proceedings of the 4th International Conference on Structures and Architecture, Lisbon, 2019.

[25] M. A. Huijbregts, Application of uncertainty and variability in LCA, The International Journal of Life Cycle Assessment 3 (5) (1998) 273.

[26] F. Pomponi, B. D'Amico, A. M. Moncaster, A method to facilitate uncertainty analysis in LCAs of buildings, Energies 10 (4) (2017) 524.

[27] R. Frischknecht, N. Jungbluth, H.-J. Althaus, G. Doka, R. Dones, T. Heck, S. Hellweg, R. Hischier, T. Nemecek, G. Rebitzer, et al., The ecoinvent database: overview and methodological framework, The international journal of life cycle assessment 10 (1) (2005) 3–9.

[28] SimaPro, Simapro 7. life cycle assessment software, Amersfoort, The Netherlands.

[29] G. Hammond, C. Jones, Inventory of carbon & energy: ICE, Vol. 5, Sustainable Energy Research Team, Department of Mechanical Engineering, University of Bath Bath, 2008.

[30] M. Lenzen, Errors in conventional and input-output—based life—cycle inventories, Journal of industrial ecology 4 (4) (2000) 127–148.

[31] R. H. Crawford, Validation of a hybrid life-cycle inventory analysis method, Journal of environmental management 88 (3) (2008) 496–506.

[32] G. Majeau-Bettez, A. H. Strømman, E. G. Hertwich, Evaluation of process-and input–output-based life cycle inventory data with regard to truncation and aggregation issues, Environmental science & technology 45 (23) (2011) 10170–10177.

[33] R. H. Crawford, P.-A. Bontinck, A. Stephan, T. Wiedmann, M. Yu, Hybrid life cycle inventory methods–a review, Journal of Cleaner Production 172 (2018) 1273–1288.

[34] F. Pomponi, M. Lenzen, Hybrid life cycle assessment (lca) will likely yield more accurate results than process-based lca, Journal of Cleaner Production 176 (2018) 210–215.

[35] R. Crawford, Life cycle assessment in the built environment, Routledge, 2011.

[36] R. Crawford, A. Stephan, F. Prideaux, P. A. Bontinck, Environmental performance in construction (EPiC), https://msd.unimelb.edu.au/research/projects/current/environmental-performance-in-construction, [Accessed: 2020-02-01] (2020).

[37] Z. S. M. Nadoushani, A. Akbarnezhad, Effects of structural system on the life cycle carbon footprint of buildings, Energy and Buildings 102 (2015) 337–346.

[38] P. Purnell, Material nature versus structural nurture: the embodied carbon of fundamental structural elements, Environmental science & technology 46 (1) (2011) 454–461.

[39] F. R. Khan, Evolution of structural systems for high-rise buildings in steel and concrete, in: Proceedings of the Regional Conference on Tall Buildings, Bratislava, Czechoslovakia, 1973.

[40] M. M. Ali, K. S. Moon, Advances in structural systems for tall buildings: emerging developments for contemporary urban giants, Buildings 8 (8) (2018) 104.

[41] Shear walls — types of shear wall and its efficiency, https://tinyurl.com/ttshoql, [Accessed: 2020-01-31] (2017).

[42] Steel frame construction hailed as key skyscraper enabler, https://tinyurl.com/yd7hcbvw, [Accessed: 2018-10-11] (2013).

[43] Construction Canada, https://tinyurl.com/yakeyp2j, [Accessed: 2018-10-11] (2017).

[44] C. Goodchild, R. Webster, K. Elliott, Economic concrete frame elements to Eurocode 2, The Concrete Centre, Camberley, Surrey, UK, 2009.

[45] B. D'Amico, F. Pomponi, Accuracy and reliability: a computational tool to minimise steel mass and carbon emissions at early-stage structural design, Energy and Buildings 168 (2018) 236–250.

[46] BS EN 1991-1-1:2002. Eurocode 1: Action on structures — Part 1-1: General actions — Densities, self-weight, imposed loads for buildings, British Standards Institution.

[47] J. Hugunin, IronPython, http://ironpython.net, [Accessed: 2018-10-09] (2012).

[48] C. Ruegg, M. Cuda, J. Van Gael, Math.Net Numerics, http://numerics.mathdotnet.com, [Accessed: 2017-09-14] (2016).

[49] BS EN 1990:2002 — Basis of Structural Design, British Standard Institution.

[50] W. McGuire, R. H. Gallagher, R. D. Ziemian, Matrix Structural Analysis, 2nd Edition, Faculty Books, 2000.

[51] BS EN 1992-1-1:2004+A1:2014. Eurocode 2: Design of concrete structures — Part 1-1: General rules and rules for buildings, British Standards Institution.

[52] BS EN 1993-1-1:2005 — Design of steel structures - Part 1-1: General rules and rules for buildings, British Standard Institution.

[53] BS EN 1995-1-1:2004+A2:2014. Eurocode 5: Design of timber structures — Part 1-1: General — Common rules and rules for buildings, British Standards Institution.

[54] D. E. Knuth, The art of computer programming, Vol. 3, Pearson Education, 1997.

[55] E. Nunez-Moreno, E. Yandzio, Steel building design: Design data "Eurocode Blue Book" (P363), SCI, Tata Steel, BCSA, 2009.

[56] Expedition engineering, the engineers toolbox, https://expeditionworkshed.org/assets/The_Engineers_Toolbox.pdf, [Accessed: 2018-10-11] (2018).

[57] J. Rackham, G. H. Couchman, S. Hicks, Composite slabs and beams using steel decking: best practice for design and construction, Metal Cladding & Roofing Manufacturers Association in partnership with the Steel Construction Institute, 2009.

[58] J. Helal, A. Stephan, R. H. Crawford, The influence of structural design methods on the embodied greenhouse gas emissions of structural systems for tall buildings, Structures 24 (2020) 650–665.

[59] BS EN 1991-1-4:2005+A1:2010-Eurocode 1. Actions on Structures. General Actions. Wind Actions, BSI, 2010.

[60] UK National Annex to BS EN 1991-1-4:2005+A1:2010-Eurocode 1. Actions on Structures. General Actions. Wind Actions, BSI, 2010.

[61] UK National Annex to BS EN 1993-1-1:2005+A1:2014-Eurocode 3. Design of steel structures Part 1-1: General rules and rules for buildings, BSI, 2005.

[62] S. M. Stigler, Gauss and the invention of least squares, The Annals of Statistics (1981) 465–474.

[63] R. Koenker, K. F. Hallock, Quantile regression, Journal of economic perspectives 15 (4) (2001) 143–156.